MITSUBISHI ELECTRIC RESEARCH LABORATORIES
http://www.merl.com

Graph-Based Array Signal Denoising for Perturbed Synthetic Aperture Radar

Liu, Dehong; Chen, Siheng; Boufounos, Petros T.

TR2020-114 July 22, 2020

Abstract

The performance of synthetic aperture radar degrades when its moving platform is perturbed with unknown position errors or received signals are interfered by strong random noise. Therefore, it is desirable to perform robust imaging with noisy radar echoes even under large position perturbations. In this paper, we propose a graph-based denoising method, which regularizes both the smoothness in the graph domain and the sparse gradients in the time domain. Different from previous GSP-based methods, our graph model is built in the radar signal domain instead of the image domain, so that we can jointly estimate position perturbations of the radar platform and denoise the received signals, providing focused imaging results. Simulation results demonstrate that our method improves the radar imaging quality from 13.3dB provided by coherence analysis to 21.6dB in terms of PSNR.

IEEE International Geoscience and Remote Sensing Symposium (IGARSS)

GRAPH-BASED ARRAY SIGNAL DENOISING FOR PERTURBED SYNTHETIC APERTURE RADAR

Dehong Liu, Siheng Chen, and Petros T. Boufounos

Mitsubishi Electric Research Laboratories
Cambridge, MA, USA

ABSTRACT

The performance of synthetic aperture radar degrades when its moving platform is perturbed with unknown position errors or received signals are interfered by strong random noise. Therefore, it is desirable to perform robust imaging with noisy radar echoes even under large position perturbations. In this paper, we propose a graph-based denoising method, which regularizes both the smoothness in the graph domain and the sparse gradients in the time domain. Different from previous GSP-based methods, our graph model is built in the radar signal domain instead of the image domain, so that we can jointly estimate position perturbations of the radar platform and denoise the received signals, providing focused imaging results. Simulation results demonstrate that our method improves the radar imaging quality from 13.3dB provided by coherence analysis to 21.6dB in terms of PSNR.

Index Terms— denoising, array signal, graph signal processing, radar platform

1. INTRODUCTION

Synthetic aperture radar uses a moving platform to form a large virtual aperture and consequently realizes high imaging resolution. However, in practice the performance of synthetic aperture radar degrades due to position perturbations of the moving radar platform and interferences to the radar echoes received by the platform. When the position perturbation level and the noise level are relatively low, one may analyze data coherence of received signals to correct phase errors caused by the perturbations [1,2] or impose sparsity on the final radar image to realize auto-focused imaging [3–5]. With the increase of perturbation and noise level, it becomes more and more challenging due to the nonconvexity of data coherence analysis. Imaging methods may be either time-consuming due to greedy search for unknown position errors, or perform poorly due to out-of-focus.

Graph signal processing (GSP) has been an active research topic in image and signal processing areas for years. GSP basically exploits the underlying specific data structure defined by the graphs [6–8] to enhance signal or image quality. Recently, GSP has been applied to synthetic aperture radar to improve the imaging performance by modeling the final radar image as a graph [9] where nodes are pixels of the radar image and edges are correlations between pixels. As a result, the radar image quality is enhanced with reduced noise. However, this image-based GSP cannot fundamentally solve the out-of-focus problem caused by radar position perturbations. Therefore, it is desirable to perform robust imaging with noisy radar echoes even under large position perturbations.

In this paper, given perturbed synthetic aperture radars with noisy radar echoes, we aim to improve the imaging performance by using a novel graph-based denosing method that can achieve position estimation and signal denoising together. We treat the synthetic aperture radar system as a graph, each transmitting and receiving position as a node of the graph, and the corresponding radar signal as the time-series associated with each node. To denoise the array signals, we formulate a graph-based objective function, which regularizes both the smoothness in the graph domain and the sparse gradients in the time domain. The main difference between our proposed method and the previous GSP-based method is that we build a graph model in the radar signal domain, instead of the image domain. We thus can jointly estimate position perturbations and denoise radar signals, providing focused imaging results. Preliminary experimental results show that the proposed method significantly improves the denoising performance combining with a robust decomposition method to estimate the position perturbation.

2. ARRAY DATA COLLECTION

We consider a 2D radar imaging problem for simplicity in which a mono-static moving radar platform is utilized to detect localized targets situated in a ROI. We use $p(t)$ and $P(\omega)$ to denote the transmitted time-domain source pulse and its frequency spectrum respectively, where

$$P(\omega) = \int_{\mathbb{R}} p(t) \mathrm{e}^{-\mathrm{j}\omega t} \, \mathrm{d}t. \tag{1}$$

Without loss of generality we assume there are up to M localized targets, each corresponds to a phase center located in the ROI. Let $\boldsymbol{l}_m$ be the location of the m^{th} target. Ideally, the mono-static radar performs as a uniform linear array, with the i^{th} radar position located at $\boldsymbol{r}_i$, for $i = 1, 2, ...N$. Due to position perturbations, the actual measurements are taken at $\widetilde{\boldsymbol{r}}_i = \boldsymbol{r}_i + \boldsymbol{\varepsilon}_i$, where $\boldsymbol{\varepsilon}_i$ stands for the unknown position perturbation of the i^{th} radar position. The overall signal received by the perturbed array is then a superposition of scattered waves from all targets in the ROI. We consider measurements at discrete frequency ω_k, where $k = 1, 2, ..., K$. After range compression, we achieve the radar measurement in the frequency domain, an $N \times K$ data matrix $\boldsymbol{Y} = [\boldsymbol{Y}_{i,k}]$ with

$$\boldsymbol{Y}_{i,k} = \sum_{m=1}^{M} |P(\omega_k)|^2 S(\omega_k, \boldsymbol{l}_m) a^2(\widetilde{\boldsymbol{r}}_i, \boldsymbol{l}_m) \mathrm{e}^{-\mathrm{j}\omega_k \frac{2\|\widetilde{\boldsymbol{r}}_i - \boldsymbol{l}_m\|}{c}} + \nu, \tag{2}$$

where $S(\omega_k, \boldsymbol{l}_m)$ is a complex-valued function of frequency ω_k and it accounts for scattering strength of the m^{th} target located at $\boldsymbol{l}_m$; $a^2(\widetilde{\boldsymbol{r}}_i, \boldsymbol{l}_m)$ accounts for the overall magnitude attenuation caused by the antenna beam-pattern and the propagation between $\boldsymbol{r}_i$ and $\boldsymbol{l}_m$; $\mathrm{e}^{-\mathrm{j}\omega_k\|\widetilde{\boldsymbol{r}}_i - \boldsymbol{l}_m\|/c}$ is the phase change term of the received signal relative to the source pulse; and ν is the overall noise. For the i^{th} radar position, $\boldsymbol{Y}_i$ is the frequency-domain measurement and $y_i(t) = \sum_{k=1}^{K} \boldsymbol{Y}_{i,k} \mathrm{e}^{2\pi\mathrm{j}\omega_k t}$ is the time-domain measurement.

Note that in applications of radar target detection, radar measurements have distinct properties: slow transition in the frequency domain and sparse gradients in the time domain. The physical mechanism is as follows. Since both the scattering strength of targets and the antenna beam-pattern change gradually in the spatial domain, the scattered electromagnetic field of ROI will also be smooth in the spatial domain. When there are several isolated targets located in the ROI, each target will generate a response or signature to radar excitation. Therefore, the time-domain gradient of radar measurement at each position will be sparse, and the sparsity level is related to the total number of targets.

3. GRAPH-BASED DENOISING

To reduce the influence of noise and position perturbations, we treat the synthetic aperture radar as a graph $G = (V, \boldsymbol{A})$, where $V = \{v_1, ..., v_i, ..., v_j, ..., v_N\}$ is the set of nodes, represented by sequential positions of the moving radar platform, and $\boldsymbol{A} \in \mathcal{R}^{N\times N}$ is the graph shift, or a weighted adjacency matrix that represents the pairwise proximity between nodes, radar signal $\boldsymbol{Y}_i \in \mathcal{C}^K$ is then the noisy time-series associated with the i^{th} node of the graph. We can estimate the graph shift through the raw measurements as

$$\boldsymbol{A}_{i,j} = \frac{|\boldsymbol{Y}_i^H \boldsymbol{Y}_j|}{\sqrt{\boldsymbol{Y}_i^H \boldsymbol{Y}_i}\sqrt{\boldsymbol{Y}_j^H \boldsymbol{Y}_j}}, \text{ for } |\boldsymbol{r}_i - \boldsymbol{r}_j| \leq R \tag{3}$$

where H indicates the Hermitian transpose, and R is the maximum distance of connected neighborhood nodes in the graph. The intuition is that when radar measurements are taken in nearby positions, the measurements should have strong pairwise correlations in the frequency domain.

Let $\boldsymbol{X}$ and $x(t)$ be the denoised frequency-domain signal and time-domain signal, respectively. To denoise radar measurements, we consider a graph-based optimization problem

$$\begin{aligned} \min_{\boldsymbol{X}, \boldsymbol{T}} \quad & \frac{1}{2}\|\boldsymbol{X} \odot \boldsymbol{T} - \boldsymbol{Y}\|_F^2 + \frac{\lambda}{2}\|\boldsymbol{X} - \bar{\boldsymbol{A}}\boldsymbol{X}\|_F^2 \\ & + \beta \sum_{i=1}^{N} |\nabla_t x_i(t)|_1, \end{aligned} \tag{4}$$

where λ, β are hyperparameters, $\odot$ stands for the element-wised product, $\boldsymbol{T} = [e^{-\mathrm{j}t_i\omega_k}] \in \mathcal{C}^{N\times K}$, which compensates the time shift misalignment caused by position perturbations, $\nabla_t x_i$ represents the gradient of the time series x_i associated with the i^{th} node, and $\bar{\boldsymbol{A}}$ is a normalized graph shift matrix whose entries are computed as $\bar{\boldsymbol{A}}_{i,j} = \boldsymbol{A}_{i,j}/\sum_j \boldsymbol{A}_{i,j}$ to ensure each row of $\bar{\boldsymbol{A}}$ sum up to 1. The intuition behind the optimization problem (4) is that we optimize over both the radar signals $\boldsymbol{X}$ and position perturbations $\boldsymbol{T}$, achieving joint signal denoising and position perturbation estimation.

The objective function in (4) includes three terms. The first term represents signal fidelity term with the appropriate time shift t_i to compensate the phase misalignment of the i^{th} position perturbation. The second term is the ℓ_2-norm graph total variation of denoised signal $\boldsymbol{X}$, which is widely used in the graph signal processing [8]. The graph total variation

$$\|\boldsymbol{X} - \bar{\boldsymbol{A}}\boldsymbol{X}\|_F^2 = \sum_i \|\boldsymbol{X}_i - \sum_{j\in\mathcal{N}_i} \bar{\boldsymbol{A}}_{i,j}\boldsymbol{X}_j\|_2^2$$

compares the difference between the radar measurements associated with each node and the weighted average of its neighbors. Minimizing this term promotes the graph smoothness; that is, neighbouring nodes should share similar radar measurements in the frequency domain. The third term is the ℓ_1-norm total variation of the time-domain signal x_i. It promotes the sparse gradients in the time domain. Overall, we use dual regularization terms to capture the physical properties of radar measurements for target detection.

To solve the optimization problem (4), we alternately update the denoised signal $\boldsymbol{X}$ and the time shift t_i due to position perturbations.

To optimize $\boldsymbol{X}$, we fix the time shift t_i for $i = 1, ..., N$. According to the signal processing theory, we can rewrite $\nabla_t x_i$ as

$$\nabla_t x_i(t) = \boldsymbol{F}^{-1}\left([\mathrm{j}\omega_k] \odot \boldsymbol{X}_i\right),$$

where $\boldsymbol{F}^{-1}$ is the inverse Fourier transform. We solve $\boldsymbol{X}$ through soft-thresholding the closed-form solution of the two quadratic terms. The denoised signal at the i^{th} node is

$$\widehat{\boldsymbol{X}}_i = [\frac{1}{\mathrm{j}\omega_k}] \odot \boldsymbol{F}\left\{S_\beta\left[\boldsymbol{F}^{-1}\left([\mathrm{j}\omega_k] \odot \tilde{\boldsymbol{X}}_i\right)\right]\right\},$$

where the soft-thresholding operator S_β is defined as

$$S_\beta(z) = \max(|z| - \beta, 0)z/|z|,$$

and

$$\tilde{\boldsymbol{X}} = \left(\boldsymbol{I} + \lambda(\boldsymbol{I} - \bar{\boldsymbol{A}})^T(\boldsymbol{I} - \bar{\boldsymbol{A}})\right)^{-1}(\boldsymbol{Y} \odot [e^{\mathrm{j}t_i\omega_k}]).$$

To optimize the time shift t_i for $i = 1, ..., N$, we fix the estimated signals $\boldsymbol{X}_i = \widehat{\boldsymbol{X}_i}$. The time shift t_i can be estimated by

$$\widehat{t_i} = \underset{t}{\operatorname{argmax}} \sum_t \left[(\boldsymbol{X}_i^H)^T \odot \boldsymbol{Y}_i \odot e^{-\mathrm{j}t\omega_k}\right], \tag{5}$$

which can be implemented by the inverse Fourier transform. Note that $\boldsymbol{Y}$ is noisy and the estimation of t_i is not convex. Therefore, t_i using (5) maybe not accurate. In order to improve the accuracy of the time shift t_i, we use cross validation

$$t_{i,j} = \underset{t}{\operatorname{argmax}} \sum_t \left[\left((\boldsymbol{X}_i \odot e^{-\mathrm{j}t_i\omega_k}\right)^H\right]^T \odot \left[\boldsymbol{X}_j \odot e^{-\mathrm{j}t_j\omega_k}\right] \odot e^{-\mathrm{j}t\omega_k} \tag{6}$$

to form a time shift matrix $\boldsymbol{\Phi} = [t_{i,j}]$, where $t_{i,j}$ represents the time shift between radar signal measured at i^{th} and j^{th} positions due to position perturbations.

Let $\boldsymbol{\varphi} = [t_1, t_2, ..., t_N]^T$ and $\boldsymbol{L}(\boldsymbol{\varphi}) = \boldsymbol{\varphi}\mathbf{1}^T - \mathbf{1}\boldsymbol{\varphi}^T$. Ideally, we have $t_{i,j} = t_i - t_j$, i.e., $\boldsymbol{\Phi} = \boldsymbol{L}(\boldsymbol{\varphi})$, where $\boldsymbol{L}(\boldsymbol{\varphi})$ is a low-rank matrix of rank not great than two. However, due to noisy measurement, the time shift matrix acquired by (6) is not a low rank matrix. Inspired by the robust principal component analysis [10], we achieve $\boldsymbol{\varphi}$ by decomposing the time shift matrix $\boldsymbol{\Phi}$ into a low-rank matrix and a sparse matrix as

$$\min_{\boldsymbol{\varphi}, \boldsymbol{S}} \frac{1}{2}\|\boldsymbol{\Phi} - \boldsymbol{L}(\boldsymbol{\varphi}) - \boldsymbol{S}\|_F^2 + \gamma\|\mathrm{vec}\{\boldsymbol{S}\}\|_1, \tag{7}$$

where γ is a hyperparameter, and $\boldsymbol{S}$ represents a sparse matrix which absorbs spike errors in the time shift matrix. Similar to (4), the above equation (7) can be solved by a least-squares solution followed by a soft-thresholding process. Once $\boldsymbol{\varphi}$ is achieved by solving (7), the time shift t_i is straightforward according to $\boldsymbol{\varphi} = [t_1, t_2, ..., t_N]^T$. The position perturbation at the i^{th} radar position is then estimated by $|\varepsilon_i| = \frac{t_i c}{2}$.

4. SIMULATION RESULTS

The simulation setup is depicted in Fig. 1, where the black dots indicate ideal moving radar positions, and x-marks to indicate perturbed radar positions. We use a differential Gaussian pulse to illuminate the region of interest (ROI), as indicated by the dashed rectangle, to detect targets represented by four black dots in the ROI. The received signals are simulated using (2) with added white Gaussian noise. Fig. 2(a) shows the simulated noisy signal whose peak-signal-to-noise ratio (PSNR) is 10dB.

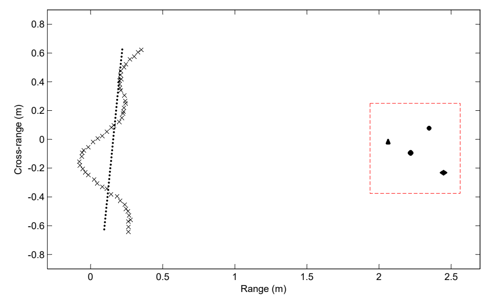

Fig. 1. Simulation setup for radar data collection.

In our graph-based denoising method, we choose $\lambda = 10^{PSNR/20+1}$, where PSNR is our estimated data peak signal-to-noise ratio in dB, $\beta = 0.15 \max|x(t)|$, and $\gamma = 0.05 \times 10^{-9}$. We present the denoised graph signal using our proposed method in Fig.2(b), from which we see that radar echoes from targets are much clearer than the noisy one. A further quantitative analysis shows that the PSNR is improved from 10dB to 20.2dB. With time compensation, the denoised signal are well aligned as shown in Fig.2(c). The corresponding position perturbations are also estimated, and compared with that estimated by coherence analysis [4]; see Fig. 3. We notice that the estimated positions using our proposed method matches the true perturbed positions well. However, the position estimates based on coherence analysis exhibit large errors. This is because data coherence-based perturbation estimation is unstable due to the noisy data.

With the denoised radar signal, we perform radar imaging; see in Fig.4 (a). For comparison, the imaging result based on coherence analysis is shown in Fig.4 (b). It is clear that our proposed method generates a sharper image with less background noise than the coherence-based method does. By defining image patches of targets as the signal and the remaining areas as the background noise, we compute PSNRs of these two radar images. The PSNRs of the graph-based radar image and the coherence-based radar image are 21.6dB and 13.3dB respectively, meaning 8.3dB improvement of our proposed method. We have examined our method on other scenarios of different target positions and different perturbed radar positions, all with consistent outperformed results[1].

5. CONCLUSIONS

We proposed a graph-based algorithm to denoise array signals collected by a perturbed synthetic aperture radar. Our method performs joint radar signal denoising and radar perturbation estimation by using a dual-regularization-based optimization. Simulation results demonstrate that our proposed method improves the imaging performance by more than 8dB of PSNR.

[1] Due to the space limit, we cannot show all the results here.

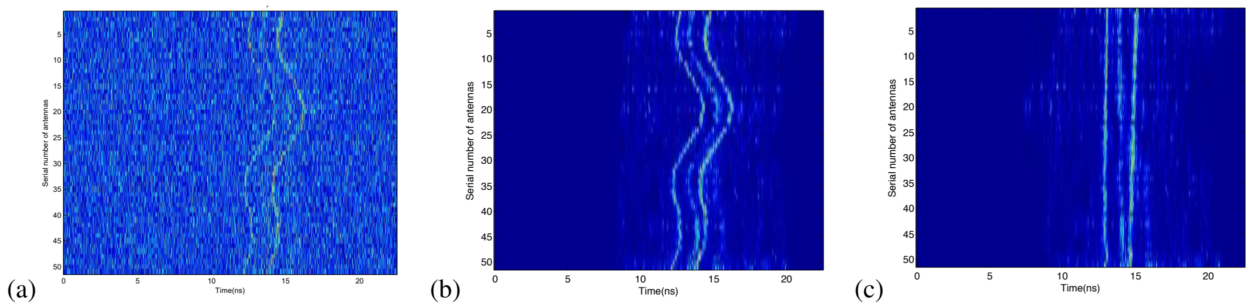

Fig. 2. Time-domain radar signals: (a) Original noisy data $y_i(t)$, (b) Denoised data $x_i(t + t_i)$ using proposed method, and (c) Denoised and aligned data $x_i(t)$ after time compensation.

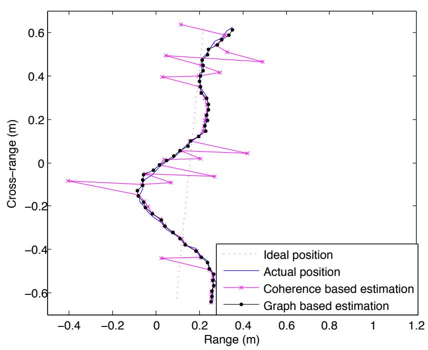

Fig. 3. Comparison between actual perturbed radar positions and estimated positions.

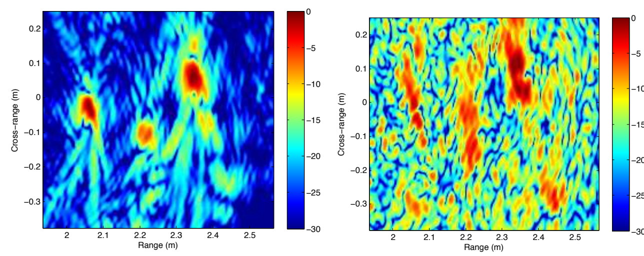

(a) Proposed method. (b) Coherence analysis.

Fig. 4. Comparison of radar imaging results. The proposed graph-based method improves the radar imaging quality from 13.3dB given by the coherence analysis to 21.6dB.

6. REFERENCES

[1] DE Wahl, PH Eichel, DC Ghiglia, and CV Jakowatz, "Phase gradient autofocus - a robust tool for high resolution SAR phase correction," *IEEE Transactions Aerospace and Electronic Systems*, vol. 30, no. 3, pp. 827–835, 1994.

[2] Fabrizio Berizzi, Marco Martorella, Andrea Cacciamano, and Amerigo Capria, "A contrast-based algorithm for synthetic range-profile motion compensation," *IEEE Transactions Geoscience and Remote Sensing*, vol. 46(10), pp. 3053–3062, October 2008.

[3] N Özben Onhon and Müjdat Cetin, "A sparsity-driven approach for joint SAR imaging and phase error correction," *IEEE Transactions Image Processing*, vol. 21(4), pp. 2075–2088, April 2012.

[4] Dehong Liu, Ulugbek S Kamilov, and Petros T Boufounos, "Coherent distributed array imaging under unknown position perturbations," in *2016 4th International Workshop on Compressed Sensing Theory and its Applications to Radar, Sonar and Remote Sensing (CoSeRa)*. IEEE, 2016, pp. 105–109.

[5] Hassan Mansour, Dehong Liu, Ulugbek S Kamilov, and Petros T Boufounos, "Sparse blind deconvolution for distributed radar autofocus imaging," *IEEE Transactions on Computational Imaging*, vol. 4, no. 4, pp. 537–551, 2018.

[6] Aliaksei Sandryhaila and Jose MF Moura, "Big data analysis with signal processing on graphs," *IEEE Signal Processing Magazine*, vol. 31, no. 5, pp. 80–90, 2014.

[7] Antonio Ortega, Pascal Frossard, Jelena Kovačević, José MF Moura, and Pierre Vandergheynst, "Graph signal processing: Overview, challenges, and applications," *Proceedings of the IEEE*, vol. 106, no. 5, pp. 808–828, 2018.

[8] Siheng Chen, Aliaksei Sandryhaila, José MF Moura, and Jelena Kovačević, "Signal recovery on graphs: Variation minimization," *IEEE Transactions on Signal Processing*, vol. 63, no. 17, pp. 4609–4624, 2015.

[9] Shahzad Gishkori and Bernard Mulgrew, "Graph signal processing-based imaging for synthetic aperture radar," *IEEE Geoscience and Remote Sensing Letters*, 2019.

[10] Emmanuel J Candès, Xiaodong Li, Yi Ma, and John Wright, "Robust principal component analysis?," *Journal of the ACM (JACM)*, vol. 58, no. 3, pp. 11, 2011.